Imperfect surface order and functionalization in vertical carbon nanotube arrays probed by near edge X-ray absorption fine structure spectroscopy (NEXAFS)

Tirandai Hemraj-Benny,[a] Sarbajit Banerjee,†[a] Sharadha Sambasivan,[b] Daniel A. Fischer,[b] Gyula Eres,[c] Alexander A. Puretzky,[c] David B. Geohegan,[c] Douglas H. Lowndes,[c] James A. Misewich[d] and Stanislaus S. Wong*[ad]

Received 9th May 2006, Accepted 25th August 2006
First published as an Advance Article on the web 8th September 2006
DOI: 10.1039/b606596c

Probing surface order as well as the degree of structural modification in carbon nanotube systems is of fundamental importance for incorporation of these materials into practical functional devices. The current study pertains to the analysis of the surface order of vertically-aligned single-walled and multi-walled carbon nanotube arrays of varying length and composition by means of near-edge X-ray fine structure spectroscopy (NEXAFS). Both NEXAFS and scanning electron microscopy (SEM) studies concluded that the nanotubes in these samples were oriented vertically to the plane of the surface. However, NEXAFS polarization analysis provided a more quantitative and nuanced description of the surface structure, indicative of far less localized surface order, an observation partially attributed to misalignment and bending of the tubes. Moreover, it was demonstrated by NEXAFS that the surface order of the arrays was imperfect and relatively independent of the height of the nanotube arrays. In addition, we have shown that NEXAFS can be used to correlate the extent of chemical functionalization and oxygenation with disruption of the electronic and physical structure of nanotubes embedded in array motifs.

1. Introduction

One main advantage of using carbon nanotubes with their promising size-dependent electronic properties is that as spatially constrained one-dimensional structures, they are the smallest dimensional systems that can be used for the efficient transport of electrons and hence are expected to be particularly important in the construction and integration of nanoscale devices. For instance, attempts have been made to organize nanotubes into highly ordered arrays for electronic and photonic applications such as data storage devices and logic transistors.[1–3] Due to their excellent field emission properties, nanotubes, vertically aligned into arrays, can conceivably be incorporated into flat panel displays. Moreover, the exceptional mechanical properties[4] of these arrays should also find usage in composite materials. The point is that in order to take advantage of this diverse range of potential applications, it is extremely important to understand the chemistry, surface order, and structural integrity of arrays of nanotubes so as to make them more amenable to rational and predictable manipulation.[5] In particular, for applications, such as field emission devices, the structure and alignment of exposed tips of arrays of the constituent nanotubes are critically important.

However, it is generally difficult to determine the order and alignment of carbon nanotubes, especially at the surfaces or ends of these structures. In addition, it is even more problematic to simultaneously monitor the electronic structure and structural modification of the nanotubes at a molecular level. Although techniques such as polarized absorption spectroscopy, polarized microscopy, and X-ray scattering have been utilized in determining the degree of order and alignment in nanotube arrays,[6–8] these methods have shown limitations. For instance, in polarization Raman spectroscopy, the presence of charge transfer as well as the degree of aggregation in bundles and strain can greatly affect the Raman intensities of a carbon nanotube sample.[9,10] Moreover, visualization techniques, such as scanning electron microscopy (SEM), which generate mainly qualitative information about the bulk orientation and alignment of the entire array of the nanotubes, are limited in discerning precise surface orientation within the outermost $\sim$5 nm layer. That is, where NEXAFS can provide a better representation of the structure of the outermost, top surface of carbon nanotube arrays, SEM images of carbon nanotube arrays are usually limited to analysis of the outermost edges and sidewalls of arrays, and yield only qualitative data on the presence of disordered, tilted, or otherwise defective regions of nanotube arrays.

[a] *Department of Chemistry, State University of New York at Stony Brook, Stony Brook, NY 11794-3400. E-mail: sswong@notes.cc.sunysb.edu; sswong@bnl.gov*
[b] *Materials Science and Engineering Laboratory, National Institute of Standards and Technology, Gaithersburg, MD 20899*
[c] *Condensed Matter Sciences Division, Oak Ridge National Laboratory, Oak Ridge, Tennessee 37831*
[d] *Condensed Matter Physics and Materials Science Department, Brookhaven National Laboratory; Bldg. 480, Upton, NY 11973*
† Current address: Department of Applied Physics and Applied Mathematics, Columbia University, New York, NY 10027.

In this work, we present near-edge X-ray absorption fine structure (NEXAFS) spectroscopy as a complementary technique for quantitatively investigating surface order and alignment in well-defined single-walled carbon nanotube (SWNT)/multi-walled carbon nanotube (MWNT) arrays.[11] In addition, surface functionalization and integrity, associated with the extent of disruption of the intrinsic nanotube electronic structure, were simultaneously and comparatively analyzed across different sample arrays of carbon nanotubes.

NEXAFS spectroscopy[12] involves the excitation of electrons from a core level to partially filled and empty states. Changes in the intensity of the NEXAFS resonance absorption upon rotation of the sample in the *xy* plane of incidence of the polarized incident beam (Fig. 1) provide evidence for local bond orientation. In other words, θ can be defined as the angle between the direction of propagation of incident X-rays and the sample surface, as seen in the left inset of Fig. 1. We have recently demonstrated the application of NEXAFS spectroscopy as a structural probe in determining the degree of covalent sidewall functionalization in ozonized SWNTs and in oxidized multi-walled carbon nanotubes.[13,14] In addition, we have previously shown that NEXAFS spectroscopy could be used to deduce the nature of order in a wide range of carbon-based systems, including SWNT powder and SWNT films.[11] Furthermore, we have recently deduced valuable structural information about BN nanotubes using this technique.[15] Others have also characterized the electronic properties of horizontally aligned carbon nanotube films on a Si (100) substrate by means of NEXAFS with the results showing a strong dependence of the intensity of the π^* core exciton at 284.4 eV on nanotube alignment with respect to the polarization of the incident radiation.[16]

One can non-destructively identify whether a carbon nanotube sample is vertically or horizontally aligned by NEXAFS as well as the nature of that alignment. For instance, in previous work, we have observed that SWNT buckypaper behaves in a manner analogous to highly ordered pyrolytic graphite (HOPG). The angle of incidence can also be defined as the angle made between the electric field vector (which is oriented perpendicularly to the direction of propagation) and the sample normal (Fig. 1). The projection of the electric field vector onto the π^* orbitals determines the intensity of the NEXAFS π^* resonance. Hence, for SWNT buckypaper-like HOPG, the π^* resonance intensity decreases as the incidence angle increases from 20 to 90°. Moreover, as previously predicted,[11] vertically aligned arrays are now shown to evince the opposite trend, wherein the π^* intensity increases with increasing incidence angle from 20 to 90°, thereby corroborating the angular dependence of our sample data, which are related to sample orientation.

In this article, we demonstrate the following.

I. We can obtain quantitative information about order to an overall surface depth of $\sim$5 nm of various vertically aligned SWNT and MWNT array systems using NEXAFS spectroscopy. In other words, we have used NEXAFS as a localized probe to generate numerical indicators about the orientation of nanotube sidewalls and ends, data which could not otherwise be obtained using a microscopy technique such as SEM.

II. In addition, we have been able to simultaneously access the comparative extent of surface functionalization and structural integrity across different array samples by monitoring the π^* transitions, measured at the magic angle of 55°. The magic angle is unique in that there is a lack of polarization

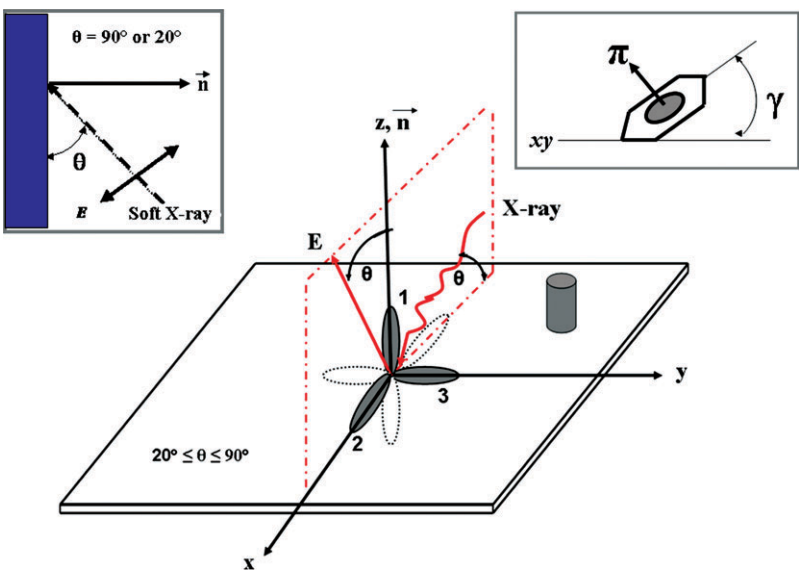

Fig. 1 Representation of π^* orbitals with respect to the electric field vector, ***E***, and the normal of the surface, ***n***. The angle of incidence changes from glancing (20°) to normal (90°) with the electric field vector oriented perpendicular to the direction of propagation in the *xz* plane. Orbitals 1 through 3 represent π^* orbitals along the *z*, *x*, *y* axes, respectively. Please see the text for further details. A typical nanotube, probed in this experimental configuration, is represented as the cylinder in the upper righthand corner of the image. For the convenience of the reader, the inset on the left denotes an alternative diagrammatic representation in two dimensions of the sample geometry with respect to the plane of incidence. The inset on the right illustrates out-of-the-plane tilts of the π system at the surface, indicated by the γ parameter, discussed more thoroughly in section 3.2.

dependence, and hence, the overall extent of surface functionalization is independent of any angular trend.

2. Experimental

The vertically aligned nanotube arrays studied were prepared using chemical vapor deposition (CVD), which was utilized to grow SWNTs and MWNTs onto evaporated metal multilayer films.[17,18] These arrays consisted of mixtures of MWNTs and SWNTs. Growth conditions were varied to generate arrays with predominantly SWNTs.[17,18] Polarized micro Raman spectroscopy on cleaved samples confirmed that the SWNTs were present throughout the length of the arrays. SEM images of a predominantly SWNT array (Fig. 2a) and of two separate mixed MWNT/SWNT arrays (Fig. 2b and c), with heights of approximately 130 microns, 1.5 mm, and 50 microns, respectively, are shown.[17,18] SEM images presented were of uncoated samples, obtained at an angle of 75°.

C K-edge partial electron yield NEXAFS spectra were taken using the U7A NIST/DOW end station at the National Synchrotron Light Source (NSLS) at Brookhaven National Laboratory. Experimental details are essentially identical to previously reported protocols.[11] The partial electron yield (PEY) signal was collected using a channeltron electron multiplier with an adjustable entrance grid bias (EGB). To eliminate the effect of incident beam intensity fluctuations and monochromator absorption features, the PEY signals were normalized using the incident beam intensity obtained from the photoemission yield of a clean Au grid with 90% transmittance. The electron yield from the top $\sim$5 nm of the arrays, *i.e.* surface as opposed to bulk sensitivity, was made possible by applying a negative bias of 50 V, wherein only Auger electrons that had suffered negligible energy loss within the sample were selected.[19] It should be noted that this signal decreases exponentially with respect to depth as described in the universal curve for the mean free path of electrons in a solid.[12]

A monochromator with a 600 line mm^{-1} grating, providing for $\sim$0.15 eV resolution, was used for all of the NEXAFS spectra collected. In addition, spectra were collected at different polarization angles by rotating the sample holder with respect to the incident beam in the plane of incidence. For the actual data collection, samples were mounted onto a stainless steel sample bar inside a UHV chamber. Samples were charge neutralized using a low energy electron flood gun, which added no noticeable background to the NEXAFS spectrum. That is, the entire sample was flooded with low energy electrons such that NEXAFS did not preferentially sample more conductive regions of the sample.

Observed changes in spectral intensity arise from anisotropy in the system and are independent of total carbon content. In general, anisotropy refers to the tendency of a material to react differently to outside fields depending on the direction the field is applied. In this particular experiment, anisotropy refers to a polarization trend observed for samples, specifically ordered carbon nanotube array samples, whereupon different intensities of partial electron yields have been noted upon irradiation at different incidence angles; these results imply that the data are correlated with geometric orientations of tubes within the samples. A comparison of intensities at different polarization angles has been made by subtracting an arctangent function to account for the C–K edge-jump and thereafter by fitting the π* resonances to a Gaussian.[11,12] Analysis of randomly oriented HiPco SWNT powder (Carbon Nanotechnologies Inc.) grown by the high-pressure CO decomposition process[20] was used to compare relative anisotropy across the various samples tested. In addition, intensities at the unique magic angle of 55° were plotted for each distinctively-treated sample in order to investigate the comparative extent of surface chemical functionalization and disruption of the nanotube's intrinsic electronic structure.

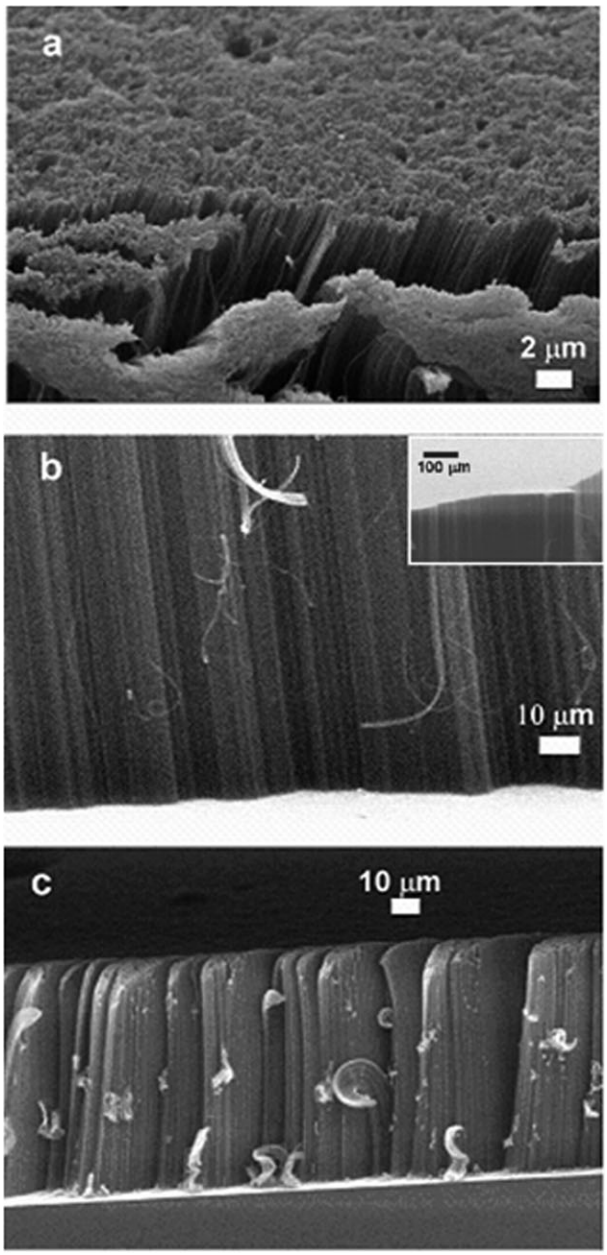

Fig. 2 SEM images of (a) 130 μm predominantly SWNT, (b) 1.5 mm SWNT/MWNT (inset showing array surface), and (c) 50 μm SWNT/MWNT arrays, respectively.

3. Results and discussion

3.1. NEXAFS data

Fig. 3 shows the variation in intensity with incidence angle for the π* and σ* resonances at the top ~5 nm surfaces of nanotube ends and tips comprising the 1.5 mm long mixed MWNT/SWNT array. Similar trends were also observed with the other two arrays but with overall varying intensities.

The spectra are characterized by a sharp C–C π* transition near 285.6 eV, a sharp σ* bound exciton near 292 eV, two other σ* transitions from 292–298 eV, and broad (σ + π) transitions from 301–309 eV.[13] In addition, features occurring in the 287–290 eV region (Fig. 3) can be assigned to oxygenated surface functionalities,[13,14] specifically corresponding to π* C═O and σ* C–O resonances.[13]

In Fig. 4, we study the diminution of the C–C π* transition near 285.6 eV and the concomitant increase in the intensity of the C–O peaks, representing the presence of oxygenated functionalities at the polarization-independent magic angle of incidence of 55°. We can deduce the structural and chemical nature of a nanotube sample (*i.e.* the more substantial the C–O resonances and the weaker the C–C π* transition, the greater the degree of surface functionalization and the lower the structural integrity of the nanotubes). From our data, one can conclude that the 130 μm predominantly SWNT array (trace a) likely consisted of the lowest quantity of surface functionalities at the ends or tips of the nanotube arrays. Hence, because it was the least functionalized, it was likely the most structurally intact sample of the three arrays studied. By contrast, the 50 μm SWNT/MWNT array sample (trace c)

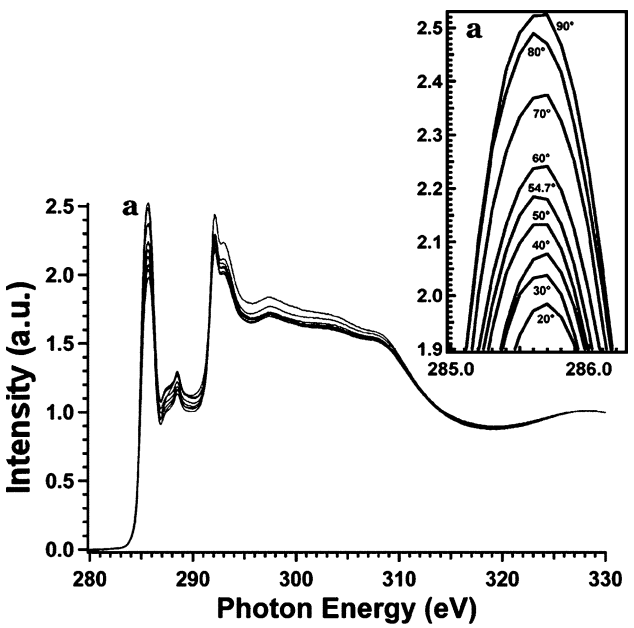

Fig. 3 Partial electron yield C K-edge NEXAFS spectra of a 1.5 mm SWNT/MWNT array taken at a retarding potential of –50 V after rotating the sample in the plane of incidence (intervals from 20 to 90°) to the incident beam. All the spectra have been pre- and post-edge normalized. Inset shows an expanded π* region. Inset: from top to bottom: data at 90, 80, 70, 60, 50, 55, 40, 30, and 20°, respectively, are shown.

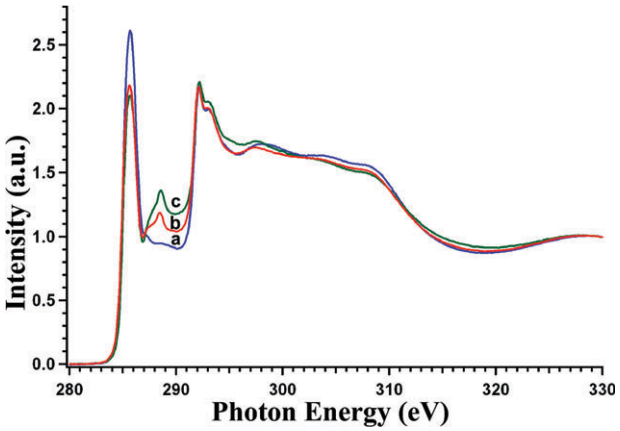

Fig. 4 Partial electron yield C K-edge spectra of (a) 130 μm predominantly SWNT (blue), (b) 1.5 mm SWNT/MWNT (red) and (c) 50 μm SWNT/MWNT arrays (green), respectively. All of the spectra have been pre- and post-edge normalized and were taken at a retarding potential of −50 V at an incidence angle of 55°.

demonstrated the greatest disruption of the π-network due to the presence of the highest degree of surface oxidation.[13] These results are important towards gaining a fundamental understanding of the nature of surface chemical composition and electronic structure of these arrays, critical for future manipulation of these samples.

In order to further confirm the nature of the alignment and to determine the degree of surface order within the uppermost 5 nm layers of the nanotubes, the intensities of integrated π* resonance peaks were analyzed in detail. Fig. 5 shows the variation in the integrated intensity of the π* resonance with angle of incidence in the three vertically aligned samples. Data for the carbon nanotube powder are shown as a comparison (black squares). The size of the error bars is based on an estimate of the typical error associated with the observed intensity of these samples. All three of the array samples were synthesized by a similar method and show comparable behavior, as was previously predicted for vertically aligned arrays of carbon nanotubes.[11]

As mentioned, if we define the incidence angle as the angle made between the incidence beam and the plane of incidence (*i.e. xy* plane), the electric field vector, ***E***, will be oriented perpendicularly to the direction of propagation (Fig. 1, left inset). The maximum NEXAFS peak intensity is observed corresponding to the maximum projection of ***E*** onto the individual orbitals. We noted that vertically oriented carbon nanotubes evinced a trend of increasing integrated π* intensity with increasing incidence angle from 20 to 90°. In addition, it was observed that the 1.5 mm SWNT/MWNT array showed the highest degree of surface anisotropy.

3.2. Defining and quantifying nanotube order using various fitting parameters

In order to quantify the extent of surface alignment in the vertically oriented arrays studied here, two different approaches for evaluating order were used, providing similar results. First, as shown in Fig. 5, a fit to a cosine function (eqn

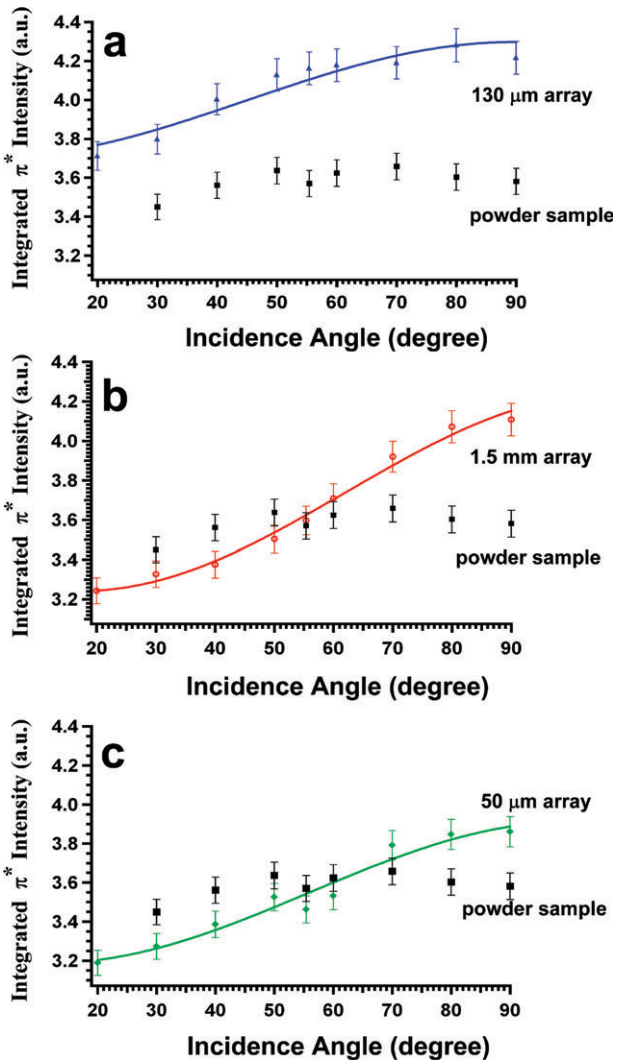

Fig. 5 Integrated intensities of π* resonances at different angles of incidence. (a) Triangles (blue) correspond to the 130 μm predominantly SWNT array, while squares (black) correspond to the SWNT powder. (b) Circles (red) correspond to the 1.5 mm SWNT/MWNT array; squares (black) correspond to the SWNT powder data. (c) Diamonds (green) correspond to data associated with the 50 μm SWNT/MWNT array; squares (black) correspond to the SWNT powder. The solid line in all cases represents a fit to the cosine function used to determine (b/a) values of normalized amplitude. All data are within ± a 2.8% error. The error bars represent goodness-of-fit parameters for the peak fitting. Further details are described in the text.

(1)) to the plot of the NEXAFS π* intensity with respect to incidence angle was performed, which gave a normalized amplitude defined as the unitless order parameter, (b/a). In theory,[21] for a three-dimensional, randomly oriented sample, where the π* orbitals can be found oriented in all planes, this value of the normalized amplitude should be close to 0. Conversely, for a highly ordered sample, where the π* orbitals tend to be oriented in one particular plane, *e.g.* the xz plane, the order parameter should be 1.

$$I(\theta) = a + b\cos(2(\theta - \gamma)) \qquad (1)$$

The absolute calculated b/a values for the 130 μm predominantly SWNT array as well as the 50 μm and the 1.5 mm mixed SWNT/MWNT arrays were 0.07, 0.10, and 0.13, respectively, within a $<2.8\%$ error. The nonzero nature of these values indicates a finite degree of alignment in these samples. No meaningful fit could be obtained for the π* data of the powder sample (black squares in Fig. 5) due to the random orientation of the tubes.

The term, γ, in eqn (1) and the right inset of Fig. 1 is known as the surface tilt angle or tube axis parameter, and represents the actual angle between the xy plane and the nanotube tips at the surfaces of the arrays. Hence, the magnitude of these values is suggestive of the degree of nanotube alignment above the substrate surface. In our case, the nanotube powder sample yielded $\gamma \approx 0^\circ$, suggestive of complete surface disorder. The 1.5 mm SWNT/MWNT array sample gave a value of $\gamma = 34 \pm 6^\circ$, indicative of a degree of non-orthogonal vertical surface alignment above the substrate and overall, of some level of misalignment. For the 50 micron MWNT/SWNT sample, we compute the value of γ to be $22 \pm 13^\circ$. Finally, for the 130 μm predominantly SWNT sample, the corresponding γ parameter is $152 \pm 5^\circ$. Based on the magnitude of these values and associated error bars involved, we can predict that the 1.5 mm, 50 micron, and 130 micron samples were not particularly well ordered, in agreement with the as-computed (b/a) values. It should be emphasized though that this angular term is largely insensitive to the overall degree of surface defects and functionalities, assuming that these are spatially randomized.

To further validate the above results, a second method, involving a $\sin^2\theta$ fit to the data, was performed, as shown in Fig. 6. Values for the dichroic ratio, $(I_{\text{perpendicular}}-I_{\text{parallel}})/(I_{\text{parallel}} + I_{\text{perpendicular}})$ with $I_{\text{perpendicular}}$ as the π* intensity for a θ value of 0° and with I_{parallel} as the π* intensity for a θ value of 90°, were obtained from an analysis similar to one previously reported.[11] That is, the value of $I_{\text{perpendicular}}$ at 0° was obtained from a linear extrapolation of the sine squared fit line for each of the samples to zero in Fig. 6. It was observed that the trend in these numbers do in fact mirror the behavior observed with the (b/a) values. In effect, the dichroic ratio values for the 130 μm SWNT array, the 50 μm SWNT/MWNT array, the 1.5 mm SWNT/MWNT array, and SWNT powder were found to be 0.08, 0.11, 0.14, and 0.03, respectively, with a $<2.8\%$ error. Thus, we can conclude the following based on values of dichroic and (b/a) ratios.

(i) Based on the relatively low values of the dichroic ratio in agreement with the (b/a) values obtained above, one can conclude from the cumulative data that the surfaces (top $\sim$5 nm) of the three sample arrays are not very well-ordered relative to the entire arrangement of tubes within each array, as depicted by SEM images.

(ii) Both order parameters suggest that the 1.5 mm SWNT/MWNT arrays showed the greatest degree of surface order amongst all of the arrays.

(iii) All three vertically aligned nanotube array samples show a higher degree of surface order in comparison with the powder samples. Moreover, these data showed that the random orientation (azimuthal disorder) of the tubes within the powder accounted for the lack of any angular dependence trend observed with the π* intensity values (Fig. 5 and 6).

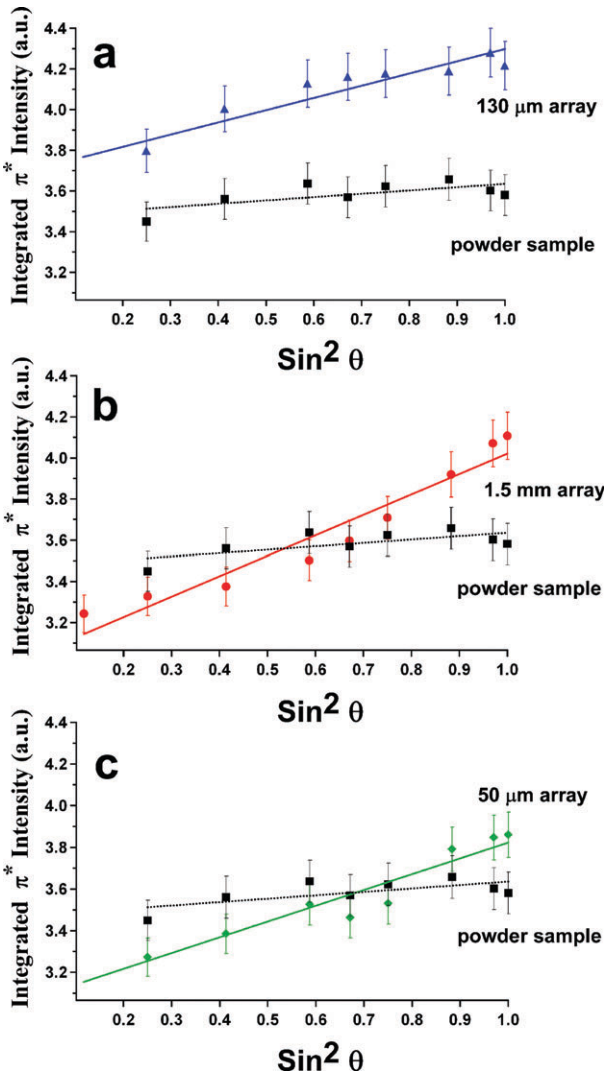

Fig. 6 Integrated intensities of π* resonances fitted to $\sin^2\theta$. (a) Triangles (blue) correspond to the 130 μm predominantly SWNT array; squares (black) designate the SWNT powder. (b) Circles (red) correspond to the 1.5 mm SWNT/MWNT array, whereas squares (black) are associated with the SWNT powder. (c) Diamonds (green) correspond to data associated with the 50 μm SWNT/MWNT array, whereas squares (black) are associated with the SWNT powder. The solid line in all cases represents a fit to sine squared theta used to determine the dichroic ratio values. All data are within a ±2.8% error. Further details are described in the text.

It can thus be concluded as a demonstration of principle that one can readily differentiate between an ordered sample and a disordered sample (in the top ~5 nm), *i.e.*, between an array of carbon nanotubes and a powder sample of carbon nanotubes, as well as between ostensibly similar vertically aligned array samples using NEXAFS. The extent of disorder will likely depend upon curvature effects, tube bending, and misalignment issues.

4. Conclusions

We have shown that NEXAFS spectroscopy can be used to determine the surface orientation and the extent of order in SWNT and MWNT vertically aligned carbon nanotube arrays grown on a substrate. This analysis provided for a complementary, more nuanced, and therefore more useful determination of local surface order as compared with SEM analyses of the same samples. That is, what may appear as a perfect surface order in microscopy is actually revealed to be imperfect using a more quantitative NEXAFS tool. These results are in agreement with prior predictions,[11] deduced from NEXAFS, regarding order and alignment in carbon nanotube buckypaper samples.

In addition, we can simultaneously determine the comparative extent of surface functionalization and structural integrity across different array samples by means of NEXAFS. From this study, it was shown that surface disorder does not necessarily correlate with the extent of chemical functionalization. For instance, the predominantly SWNT array sample showed the lowest degree of surface order, but was the least surface functionalized or oxidized. From the data, it may be implied that the presence of MWNTs in the arrays actually created a more surface ordered or 'sturdier' array. It is practically necessary to understand both the extent of surface order as well as the extent of chemical functionalization in carbon nanotube arrays so that these nanomaterials can be effectively incorporated and manipulated into future functional devices.

Acknowledgements

We thank Dr Jim Quinn (SUNY Stony Brook) for help with and discussions about SEM. We acknowledge support of this work through startup funds provided by the State University of New York at Stony Brook as well as Brookhaven National Laboratory. Acknowledgement is also made to the National Science Foundation for a CAREER award (DMR-0348239) and to the donors of the Petroleum Research Fund, administered by the American Chemical Society, for support of this research. Research was carried out in part at the National Synchrotron Light Source at Brookhaven National Laboratory, which is supported by the US Department of Energy under contract number DE-AC02-98CH10886. Research at Oak Ridge National Laboratory, managed by UT-Batelle, LLC, was sponsored under contract DE-AC05-00OR22725.

References

1 S. S. Xie, B. H. Chang, W. Z. Li, Z. W. Pan, L. F. Sun, J. M. Mao, X. H. Chen, L. X. Qian and W. Y. Zhou, *Adv. Mater.*, 1999, **11**, 1135.
2 F. Rohmond, L. K. L. Falk and E. E. B. Campbell, *Chem. Phys. Lett.*, 2000, **328**, 369.
3 P. M. Ajayan, O. Stephan, C. Colliex and D. Trauth, *Science*, 1994, **265**, 1212.
4 R. H. Baughman, A. A. Zakhidov and W. A. de Heer, *Science*, 2002, **297**, 787.
5 S. Banerjee, T. Hemraj-Benny and S. S. Wong, *Adv. Mater.*, 2005, **17**, 17.
6 M. Ichida, S. Mizuno, H. Kataura, Y. Achiba and A. Nakamura, *Appl. Phys. A*, 2004, **78**, 1117.
7 P. Launois, A. Marucci, B. Vigolo, P. Bernier, A. Derre and P. Poulin, *J. Nanosci. Nanotechnol.*, 2001, **1**, 125.
8 H. Shimoda, B. Gao, X. P. Tang, A. Kleinhammes, L. Fleming, Y. Wu and O. Zhou, *Phys. Rev. Lett.*, 2002, **88**, 015502.

9 A. Kukovecz, T. Pichler, R. Pfeiffer, C. Kramberger and H. Kuzmany, *Phys. Chem. Chem. Phys.*, 2003, **5**, 582.
10 O. Lourie and H. D. Wagner, *J. Mater. Res.*, 1998, **13**, 2418.
11 S. Banerjee, T. Hemraj-Benny, S. Sambasivan, D. A. Fischer, J. A. Misewich and S. S. Wong, *J. Phys. Chem. B*, 2005, **109**, 8489.
12 (*a*) J. Stöhr, *NEXAFS Spectroscopy*, Springer-Verlag, Berlin, 1992; (*b*) J. Stöhr, M. G. Samant, J. Lüning, A. C. Callegari, P. Chaudhari, J. P. Doyle, J. A. Lacey, S. A. Lien, S. Purushothaman and J. L. Speidell, *Science*, 2001, **292**, 2299.
13 S. Banerjee, T. Hemraj-Benny, M. Balasubramanian, D. A. Fischer, J. A. Misewich and S. S. Wong, *Chem. Commun.*, 2004, **7**, 772.
14 S. Banerjee, T. Hemraj-Benny, M. Balasubramanian, D. A. Fischer, J. A. Misewich and S. S. Wong, *ChemPhysChem*, 2004, **5**, 1416.
15 T. Hemraj-Benny, S. Banerjee, S. Sambasivan, D. A. Fischer, W. Han, J. A. Misewich and S. S. Wong, *Phys. Chem. Chem. Phys.*, 2005, **7**, 1103.
16 L. Fleming, M. D. Ulrich, K. Efimenko, J. Genzer, A. S. Y. Chan, T. E. Madey, S. J. Oh, O. Zhou and J. E. Rowe, *J. Vac. Sci. Technol., B*, 2004, **22**, 2000.
17 H. Cui, G. Eres, J. Y. Howe, A. A. Puretkzy, M. Varela, D. B. Geohegan and D. H. Lowndes, *Chem. Phys. Lett.*, 2003, **374**, 222.
18 D. B. Geohegan, A. A. Puretzky, I. N. Ivanov, S. Jesse, G. Eres and J. Y. Howe, *Appl. Phys. Lett.*, 2003, **83**, 1851.
19 J. Genzer, E. J. Kramer and D. A. Fischer, *J.Appl. Phys.*, 2002, **92**, 7070.
20 P. Nikolaev, M. J. Bronikowski, R. K. Bradley, F. Rohmund, D. T. Colbert, K. A. Smith and R. E. Smalley, *Chem. Phys. Lett.*, 1999, **313**, 91.
21 T. Sakai, K. Ishikawa, H. Takezoe, N. Matsuie, Y. Yamamoto, H. Ishii, Y. Ouchi, H. Oji and K. Seki, *J. Phys. Chem. B*, 2001, **105**, 9191.

